CORROSION SCIENCE AND TECHNOLOGY, Vol.23, No.5(2024), pp.383~392
[Research Paper]
pISSN 1598-6462 / eISSN 2288-6524
DOI: https://doi.org/10.14773/cst.2024.23.5.383

Modifying the τ5c-$Al_{20}Fe_5Si_2$(+Zn) Intermetallic Phase by Adding Vanadium into 55%Al-Zn Coating Alloy

Nega Setargew[1,†], Simon Correnti[1], Daniel Parker[1], Daniel McLachlan[1], and Dongdong Qu[2]

[1]*BlueScope Steel Innovation Labs, Port Kembla 2505, Australia*
[2]*School of Mechanical and Mining Engineering, The University of Queensland, Brisbane Qld 4072, Australia*
(Received May 31, 2024; Revised August 06, 2024; Accepted August 07, 2024)

The presence of transition metals V, Cr or Mn in a 55%Al-Zn based coating metal can modify the equilibrium intermetallic phase, τ5c, by diffusion of transition metals and substituting for iron in the τ5c phase. We experimentally confirmed the modification of the IMC phase using various analytical techniques to characterize IMC phases. Experimental results confirmed the formation of a modified τ5c-$Al_{20}(Fe,V)_5Si_2$(+Zn) intermetallic phase. The modified IMC phase showed periodic repeating layers with varying concentrations of V while still maintaining a constant (Fe+V)/Fe ratio within the homogeneity range of Fe in the equilibrium IMC phase. We proposed a reaction-diffusion mechanism for forming a modified IMC phase and a periodic layered structure. The initial reaction of the steel strip resulted in the formation of Fe_4Al_{13} IMC phase. Al, Si, and Zn diffused and reacted with Fe_4Al_{13} to form the equilibrium bcc phase, τ5c. The Fe_4Al_{13} phase was consumed in the reaction, followed by diffusion of V into the newly formed phase by substitution of Fe by V, resulting in formation of the modified IMC phase. At 600 °C, the τ5c phase could dissolve up to 4.13 wt% (2.73 at.%) V without changing its overall bcc crystal structure.

Keywords: *Modified IMC, τ5c-$Al_{20}Fe_5Si_2$(+Zn), θ-Fe_4Al_{13}, Periodic-layered-structure formation, Newton's Cradle*

1. Introduction

In 55%Al-Zn based metal coated steel both the intermetallic alloy layer and the dross intermetallic compound particles (IMCs) that accumulate in the bath are composed of the quaternary intermetallic compound phase, τ5c ($Al_{20}Fe_5Si_2$ (+Zn)). This phase is the phase that is in equilibrium with the coating bath at the process temperature of 600 °C. In a continuous 55 wt% Al-43 wt% Zn-1.5 wt% Si-0.5 wt% Fe hot dip coating bath iron will continuously dissolve when the strip enters the bath. Since the bath is already saturated with iron, the iron that is dissolving from the steel strip will precipitate forming fine dispersions of the equilibrium intermetallic compound phase. The fine IMC particles will remain suspended in the bath until they eventually reach a critical size by agglomeration and sink in the gravitational field due to the density difference between the IMCs and the melt. The settled dross particles undergo further agglomeration forming what is known as the mushy and consolidated hard dross layers at the bottom of the coating pot. If transition metals (elements in group 6, the d-block in the periodic table) such as Cr, V and Mn are present in the melt, due to the low solubility of these elements in the melt they partition to the intermetallic dross phase forming what we have identified as the modified-τ5c phase. In our previous research [1] we have described the chemical composition and the formation mechanism of the Cr modified-τ5c phase in the alloy layers of the austenitic 316L stainless steel immersed pot hardware (sink rolls, stabilizer rolls, and the sink roll arms).

The chemical and microstructural analyses of the consolidated hard bottom dross samples removed from the coating pot often show the presence of Cr or V in some of the dross samples studied. In addition to contamination of the melt from the degradation of the pot hardware, intentional addition of Cr or V in the form of Al-V and Al-Cr master alloys to the bath can also lead to significant enrichment of the dross phase by Cr and V resulting in the formation of the modified-τ5c IMC phase. In the earlier work we postulated that transition metals if present in the melt will preferential diffuse to the IMC phase and substitute for Fe in the bcc structure of the τ5c phase due to the extremely low solubility of these elements in the alloy at the process temperature. The IMC

†Corresponding author: Nega.Setargew@Bluescopesteel.com

phase is not a line compound and has a wide homogeneity range and thus is known to absorb solutes for example, Zn, Cr, V, Si in significant amounts. The substitution of Fe in α-AlFeSi intermetallic phase by quaternary additions of transitions metals has been known for a long time [2-4]. The effect of a quaternary addition such as V, Cr and Mn at very low concentration was reported to transform the crystal structure and stabilize the structure of the ternary α-AlFeSi intermetallic phase from hexagonal to cubic [2].

In a study on dispersion strengthened Al-Fe-V-Si alloys, vanadium was reported to transform ternary α-AlFeSi intermetallic phase from hexagonal to a thermally stable body-centered-cubic crystal with 138 atoms/unit cell [3]. Further evidence for the substitution hypothesis was reported in valence electron structure analysis of rapidly solidified Al-Fe-V-Si alloy that showed vanadium atoms partly or entirely replacing Fe atoms leading to thermal stability of the α-AlFeSi phase [4].

In 55%Al-Zn-Fe-Si, metal coating alloy, on the other hand, the transformation and stability of the ternary α-AlFeSi intermetallic phase to the bcc structure was achieved by the substitution of Fe by Zn. In this study, our primary objectives are as follows: first, to experimentally verify the stability of the equilibrium bcc structure if a transition metal such as V is added to the quaternary IMC phase, and second, to demonstrate that the (Fe+V):Fe ratio in the intermetallic phase can be reliably used as a quantitative indicator of the substitution of Fe by the diffusion of V into the intermetallic phase. Additionally, to propose a detailed mechanism using a suitable analogy to illustrate the formation process of the periodic and layered microstructure of the V modified-τ5c intermetallic phase.

2. Experimental Methods

The 55%Al-43%Zn-1.5%Si-0.47%Fe alloy melt was prepared in a clay graphite crucible in a resistance heated furnace from Al-3wt%Si master alloy and a special high grade (SHG) zinc ingot. Once the charge was fully melted, the furnace's set-point temperature was adjusted to 710 ºC.When the target temperature was reached, strips of cold rolled steel, grade A06 (0.06 wt% C- 0.21 wt% Mn-0.04 wt% Al, max of 0.02 wt% Si-Fe) was added to the bath to generate the intermetallic dross particles. At 710 ºC, the solubility of Fe in the bath is substantially high and is of the order or around 1.20 wt%. [5]. After holding the bath at the set temperature for ~ 96 hours, the bath temperature was lowered to 600 ºC. Since the solubility of Fe in the bath is a strong function of temperature, the solubility significantly decreases to 0.47 wt% at 600 ºC. When the bath temperature is lowered to 600 ºC, the excess Fe (0.73 wt%) that was in solution at 710 ºC precipitated and formed the metastable intermetallic compound θ-Fe_4Al_{13} and with further reaction with melt it subsequently transformed into the intermetallic compound, τ5c-$Al_{20}Fe_5Si_2$(+Zn) which is the IMC phase that is in equilibrium with the bath.

After holding the bath at temperature, a sample of the mushy dross layer was collected and examined by metallography, if the layer at the bottom of the crucible contained the dross particles. After verifying the presence of the dross IMC particles in the mushy layer, an Al-10 wt% V master alloy was added to the bath and held at 600 ºC for 120 hours. After holding for 120 hours, samples of the mushy dross layer were taken at regular intervals using 12.5 mm diameter tabular alumina tubes. Samples for metallography were prepared from dross samples held at 600 ºC for 168 to up to 840 hours.

Initial examination of the microstructure of the samples were carried out by optical metallography followed by detailed SEM/EDS analyses. We used EVO 50 SEM manufactured by Carl Zeiss AG, Germany equipped with Oxford Instruments X-act PentoFET Precision EDS detector manufactured by Oxford Instruments, UK. Further characterization of the samples was carried out by micro-XRD, using SmartLab Automated Multipurpose X-ray Diffractometer (XRD) manufactured by Rigaku, Japan. and by electron backscattering diffraction pattern (EBSP). The EBSP analysis was conducted on the bulk τ5c phase using the FEI Scios dual beam system equipped with the Oxford HKL EBSD system manufactured by Oxford Instruments, UK at accelerating voltage set to 20 kV.

The micro-XRD analysis was carried out on the Rigaku SmartLab X-ray diffractometer with the Cu-source tube operated at 45 kV and 200 mA. A φ0.5 mm beam size was chosen to illuminate two localized regions on the polished sample surface to record the XRD pattern. The 2-Theta range of the XRD pattern was recorded from 8 to 90º at a scanning rate of 1.5º/min. The TOPAS-Academic

V6 package was used to help identify the phase in the sample using the Rietveld refinement. The Durham_d8 emission profile was used to fit the Cu-source X-ray. A Pseudo Voigt function was used as the peak function to reveal the lattice parameter for the identified phases.

3. Results and Discussion

3.1 Microstructural characterization: Initial development of the microstructure of the IMCs

The initial intermetallic phase that forms when the steel strip reacts with the molten alloy is the metastable θ-Fe_4Al_{13} also designated as θ-$FeAl_3$. This reaction is followed by the formation of the equilibrium intermetallic phase, τ5c-$Al_{20}Fe_5Si_2$(+Zn).

The microstructure of the dross particles after 504 hours of reaction at temperature are shown in Figs. 1a to 1d. Analysis of the microstructure of the dross particles suggests that the τ5c IMC phase will form in two distinct ways: (i) by the diffusion of Al, Si and Zn from the molten coating bath into θ-Fe_4Al_{13} in the solid state (Figs. 1a and 1b) and (ii) through the reaction with the bath and the dissolution of θ-Fe_4Al_{13} (Figs. 1c and 1d) to form the τ5c phase.

In the second case, θ-Fe_4Al_{13} is consumed in the process and the evidence for the dissolution and fragmentation of the intermetallic phase are evident in the dross samples taken at reaction times of 168 hrs to 840 hrs. The extent of the amount of dissolution and fragmentation the IMC particles increased with the longer immersion times of 504-840 hours. In addition, the micrographs shown in Fig. 1c also suggest the dissolution and fragmentation of θ-Fe_4Al_{13} occurs predominantly at the core of the IMC, while the interfacial regions of the IMC transformed to equilibrium τ5c-$Al_{20}Fe_5Si_2$(+Zn) phase and the V-modified-τ5c-$Al_{20}Fe_5Si_2$(+Zn) phase, by the inward diffusion of Al, Si, Zn and V from the surrounding melt. The SEM/EDS analysis of the regions shown in Figs. 1a-d are summarized in Tables 1 and 2. One of the interesting and intriguing microstructural features observed is the formation a periodic-layered structure of the vanadium modified-τ5c phase which are clearly visible in the micrographs shown in Fig. 1b-d. The vanadium contents

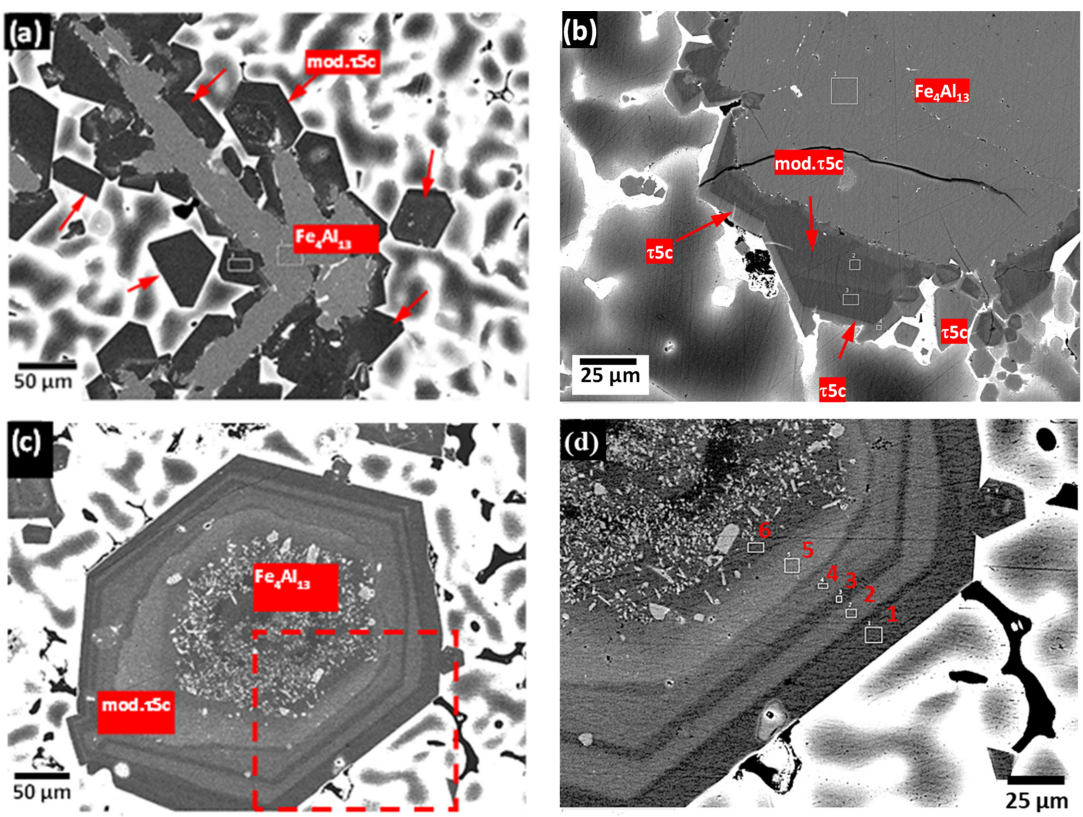

Fig. 1. The initial reactions of the A06 steel strip with bath to form θ-Fe_4Al_{13} and its transformation to the modified-τ5c intermetallic phase; Fig. 1d is higher magnification of the boxed area in Fig. 1c

of the layered structures (Table 2) show the variations in V content from the surface to the centre region of the IMC particle (labelled 1 to 6). Even though the V content of the layers varies in the periodic layers from the surface to the centre, the ratio of the (Fe+V)/Fe in the periodic-layered structures remained relatively constant from the surface to the centre of the V-modified-τ5c phase. The ratio of (Fe+V)/Fe, shown in Table 2, column 6 clearly demonstrates a steady-state diffusion process where a flux of V atoms diffuses into the bcc τ5c structure. It also signifies the constancy of the vanadium concentration gradient over time. This relationship between (Fe+V)/Fe and V is further illustrated in the plot of the line scan data from various dross samples that showed consistent linear relationship of identical magnitude irrespective of differences in the reaction times in the bath. An example of the linear plot of the (Fe+V)/Fe ratio vs V for a sample taken after 672 hours of reaction time is shown in Fig. 2b. The data plotted gives a measure of the diffusion of V into the τ5c phase in terms of the change in the relative concentration of Fe and V. Considering the plot represents an empirical relationship, inferences about the diffusion coefficient cannot be drawn from it. Instead, the relationship shown can provide a valuable insight into an effective rate of diffusion based on changes in the relative concentration of V and Fe. The empirical relationship described implies a consistent predictable change which means as the concentration of V changes the ratio of the total system concentration, (Fe+V) to the concentration of Fe changes at a constant rate.

Table 1. SEM/EDS analysis of the IMCs phases shown in Fig. 1a and 1b (wt%)

Phase	Al	Si	V	Fe	Zn
Fe_4Al_{13}	59.4	1.25	-	42.2	2.1
V mod.τ5c	56.5	5.62	2.85	29.4	5.7

3.2 Evolution of microstructure: Reaction times of 168 to 840 hours

In Figs. 3a to 3f are shown SEM backscattered electron (BSE) images of the microstructures of dross samples after 168 to 840 hours of reaction time in the bath. In the SEM/EDS analysis of the dross samples the major constituents identified in the dross phase included: the vanadium modified-τ5c-($Al_{20}Fe_5Si_2$(+Zn) IMC phases with a range of vanadium content and the reacted and

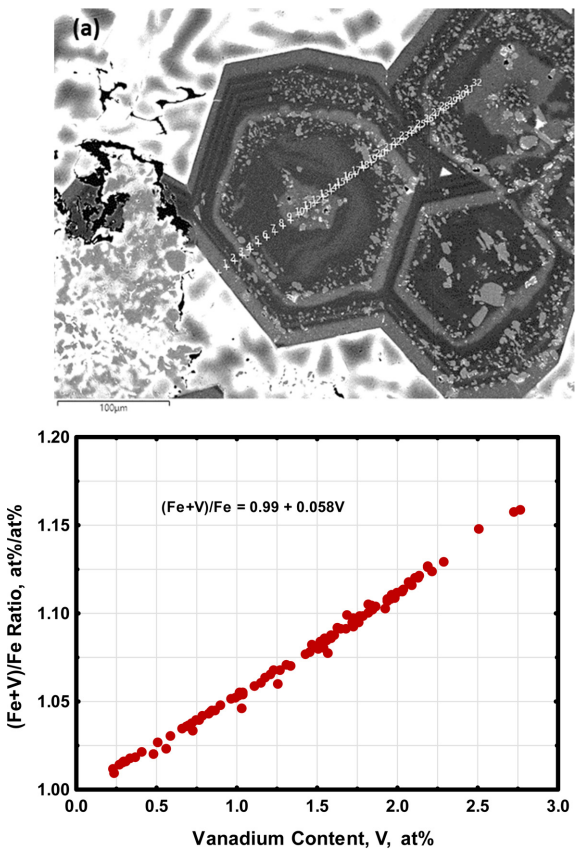

Fig. 2. An example of the dross particle used in SEM/EDS line scan (a) and (b) a plot of (Fe+V)/Fe vs V of the line scan data from several dross samples after 672 hours of reactions

Table 2. SEM/EDS analysis the periodic layered structures in Fig. 1d (wt%)

Spectrum	Al	Si	V	Fe	Zn	(Fe+V)/Fe
1	56.15	5.35	2.96	29.47	6.07	1.1
2	55.86	4.97	1.43	31.24	6.50	1.0
3	55.86	5.49	2.50	30.33	5.82	1.1
4	55.65	4.78	1.38	30.19	7.01	1.0
5	55.40	4.58	0.57	31.90	7.52	1.0
6	56.15	5.14	2.36	30.07	5.86	1.1

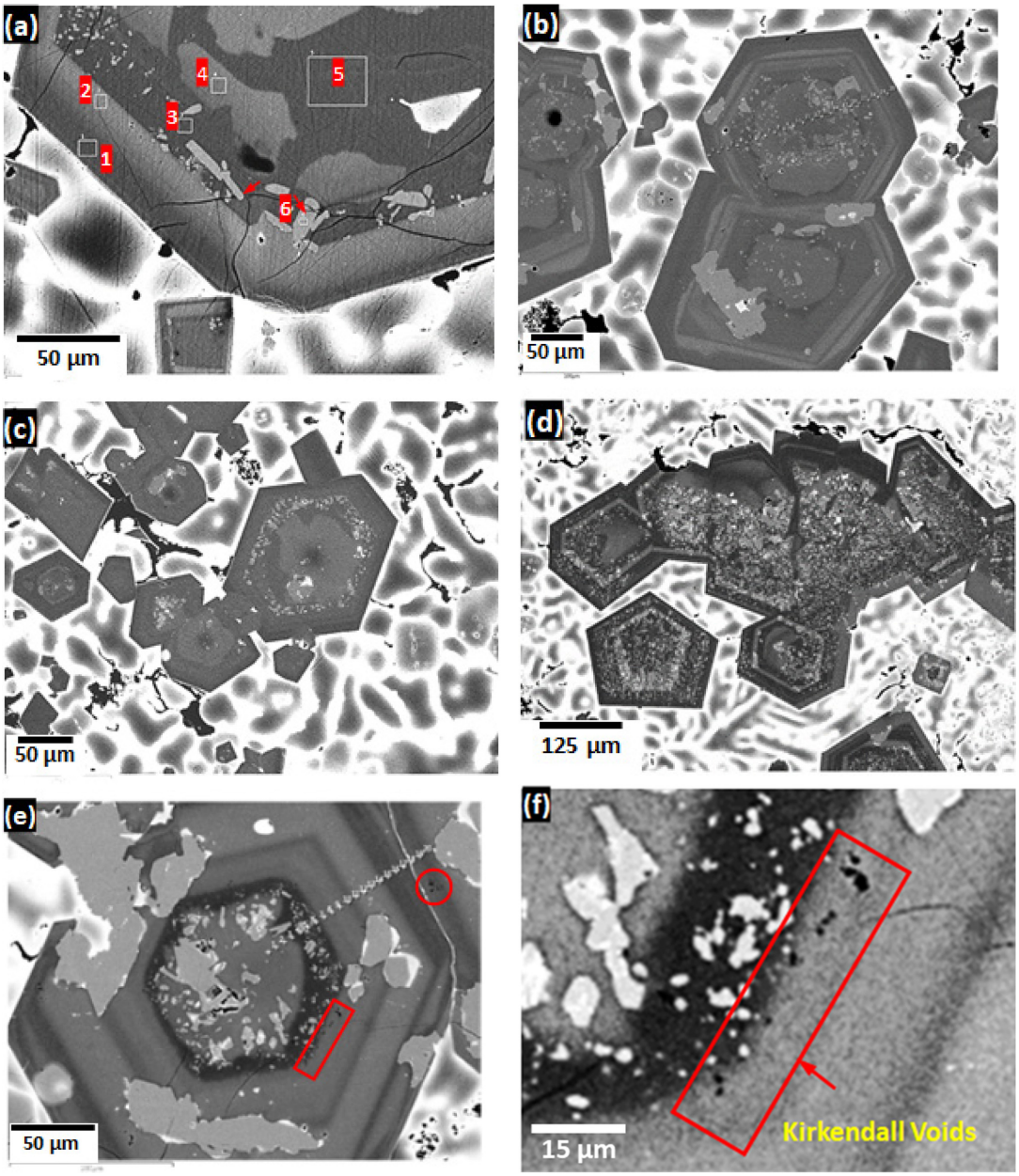

Fig. 3. SEM backscatter electron (BSE) images of the microstructures of dross samples after reaction times of: (a) 168 hours, (b) 336 hours, (c) 504 hours, (d) 672 hours, (e) 840 hours and (f) shows the presence of Kirkendall voids in the enlarged boxed area of Fig. 3e

fragmented remnants of θ-Fe_4Al_{14}. In Fig. 3a are shown the regions with varying amounts of dissolved vanadium in the V-modified τ5c phase. In the BSE images the darker regions are rich in V and the light grey areas are richer in Fe. In the analysis of numerous particles from the range of reactions times, the monoclinic crystal, θ-Fe_4Al_{14} dissolves only a minimal amount of V, approximately 0.5 wt% (0.3 at%) (spectrum 6 in Table 3). Even with extended reaction times vanadium was rarely detected in θ-Fe_4Al_{13} in most instances. The SEM/EDS analysis results of the dross particle after 168 hours of reaction (Fig. 3a) are summarized in Table 3. At the early stages of the reaction, the V-modified τ5c phases with both high and low V contents (regions 4 and 5 in Fig. 3a) at the centre of the dross particles appear irregular in shape and do not display the regular symmetrical layered structure compared with the external regions of the particle.

With increases in the reaction time, the dissolution and

Table 3. SEM/EDS analysis the periodic layered structures in Fig. 3a (wt%)

Spectrum	Al	Si	V	Fe	Zn	(Fe+V)/Fe
1	56.2	6.3	3.34	28.7	5.5	1.1
2	55.4	4.9	0.58	31.3	7.9	1.0
3	56.1	5.8	3.4	29.5	5.1	1.1
4	55.7	5.2	0.96	31.3	6.9	1.0
5	56.7	5.7	3.15	29.2	5.3	1.1
6	54.6	1.5	0.48	41.3	2.1	1.0

fragmentation of θ-Fe-Fe_4Al_{13} to finer particles is evident (Fig. 3b-e). One of the interesting microstructural characteristics observed in the agglomerated dross particles (Fig. 3), is their tendency to adopt the hexagonal form. Even the fragmented and dissolving particles of θ-Fe_4Al_{13} seem to adopt the hexagonal shape (Figs. 3d-e). The adoption of the minimum surface energy of configuration of the hexagons enhances the most transformation by diffusion for least expense in boundary/surface energy. Among regular polygons, hexagons have the smallest boundary length per unit area as well as a 6-fold rotational symmetry that can tesselate. The dross particle that had been in the bath for 840 hours, displays a well-defined overall hexagonal geometry both in its overall form and within the periodically layered structures, with varying concentrations of vanadium (Fig. 3e). In Fig. 3e at the interface between the inner darker region and the adjacent light grey layer (the rectangular boxed area), are displayed a line of porosity which are most likely Kirkendall voids.

A higher magnification micrograph of the boxed area is shown in Fig. 3f. The dark region contains 3.0 wt % (2.3 at.%) V, and the region adjacent to it contains 1.3 wt% (0.8 at.%) V.

Over time, as more vanadium diffuses into each adjoining layer, the vanadium concentration of the layers will oscillate maintaining a constant (Fe+V)/Fe ratio, the position of the Kirkendall voids may not indicate the direction of the unbalanced diffusion rate (refer to Section 4 for detailed explanation).

3.3 EBSD and Micro XRD analysis

3.3.1 EBSP analysis

Further detailed characterization of the V-modified-τ5c was carried using the electron backscattering pattern analysis on one of the outer layers of the layered structures

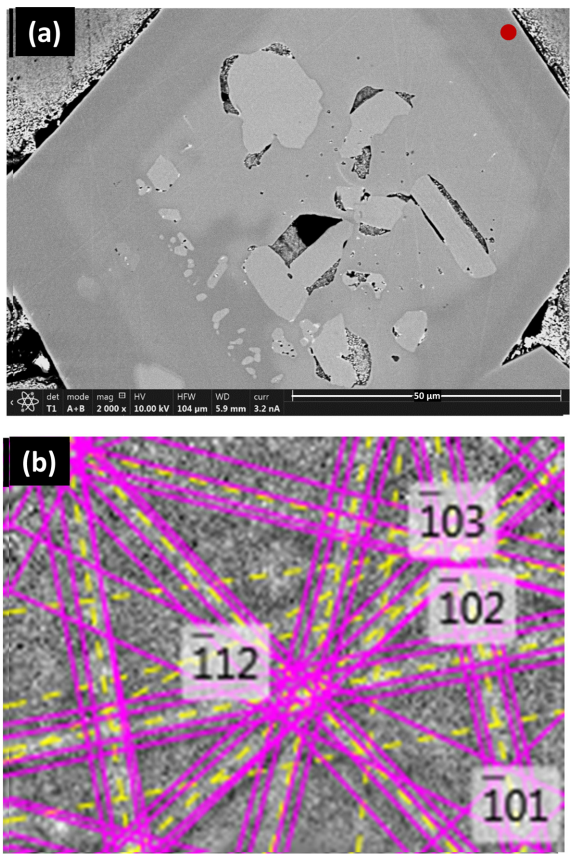

Fig. 4. The EBSP analysis of the V-modified-t5 particle (a) the red marking showing the site of the EBSP analysis, and (b) shows four different poles for the bcc lattice structure of τ5c have been automatically indexed

of the dross particle. The site of the EBSP analysis region is shown with a red dot in Fig. 4a. A body centred cubic (bcc) lattice structure with a = 12.58 Å in space group No. 204, I m-3 was used to identify the τ5c phase. A Kikuchi pattern in Fig. 4b clearly demonstrates the bcc lattice structure in the V-modified-τ5c phase. Four poles (zone axes) for this bcc lattice structure were identified: ($\bar{1}12$), ($\bar{1}03$), ($\bar{1}02$) and ($\bar{1}01$).

3.3.2 Micro XRD analysis

The micro-XRD analysis was carried out on two localized regions where the two X-ray illuminated regions are indexed by points 1 and 2. In the experiment, the position of point 1 is set to be (0, 0, 0), and the position of point 2 is determined to be (0.858, -0.9775, 0). The distance between points 1 and 2 was 1.3 mm. This distance avoids the possible overlapping of information that could

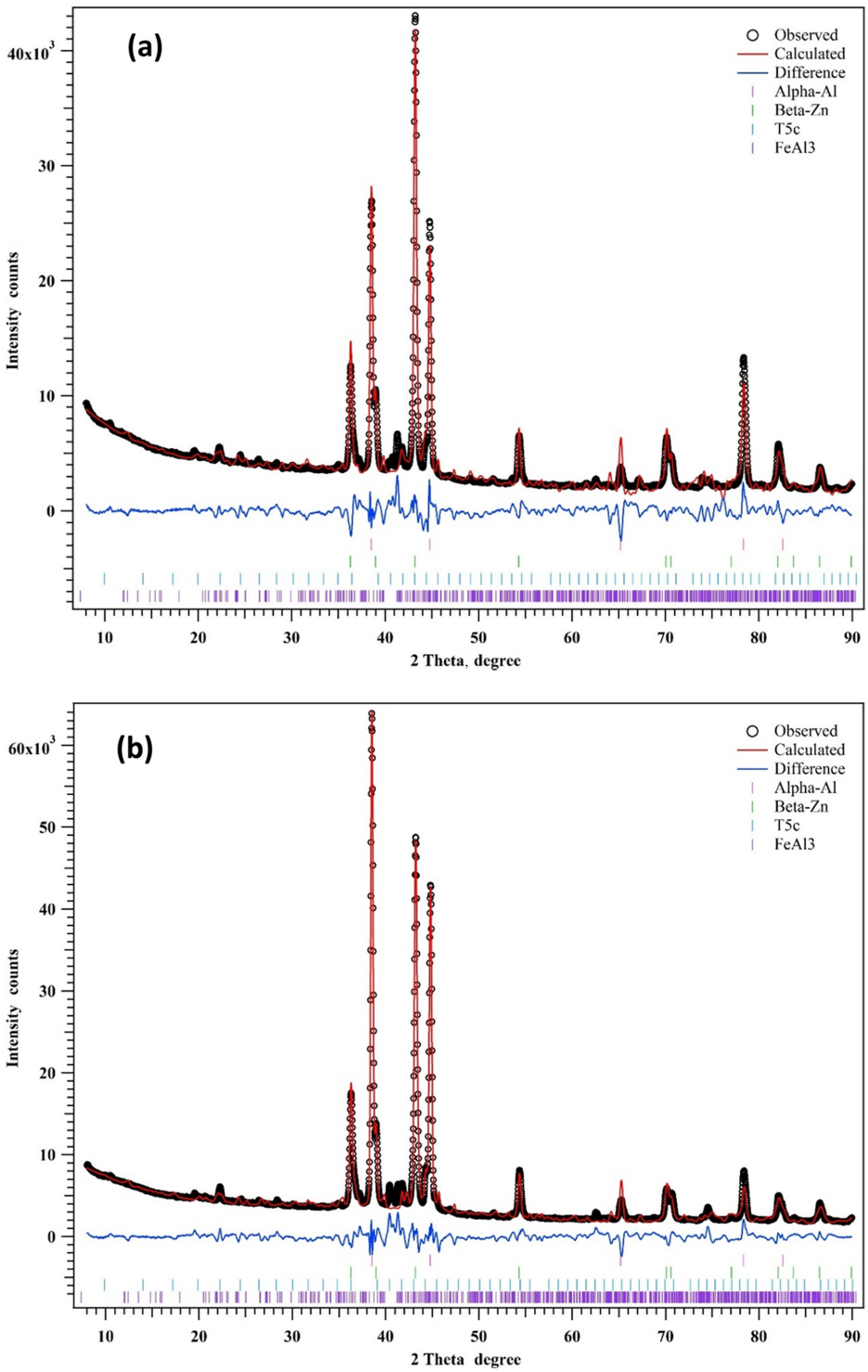

Fig. 5. Micro-XRD patterns for two regions, (a) region 1 and (b) region 2 on a polished sample of the V-modified τ5c-$Al_{20}Fe_5Si_2$(+Zn) dross particle

be recorded in the two micro-XRD patterns (Figs. 5a and 5b). The dark circles represent the observed XRD patterns. are plotted by dark circles. We found four crystalline phases in the studied sample, α-Al, β-Zn, τ5c and Fe_4Al_{13}.

Phase identification of the α-Al, β-Zn and Fe_4Al_{13} was carried out using the PDF-4+ 2018 database of the International Centre for Diffraction Data (ICDD). The PDF cards for α-Al, β-Zn and Fe_4Al_{13} are PDF 00-004-0787, PDF 00-004-0831 and PDF 00-047-1420, respectively.

The crystal structure information of τ5c body-centred cubic (bcc) lattice of 1.256 nm in space group Im-3 (space group No. 204) [6]. We used this data as the initial lattice size for the refinement of the τ5c lattice parameters. Tables 4.1 and 4.2 show the phase fractions and the refined lattice sizes for α-Al, β-Zn, τ5c and Fe_4Al_{13}, respectively. It shows that α-Al contributes the largest amount of the phase in the currently studied sample, 42.89 wt% and 68.22 wt% in regions 1 and 2, respectively, despite the phase fractions in the localized regions 1 and 2 being different. The phase fractions for β-Zn are relatively low, 7.79 wt% and 5.07 wt%. This indicates a small amount of the eutectic Al/Zn microstructure in the current sample. The phase fractions for τ5c are fitted to be 22.03 wt% and 12.79 wt%, as well as 27.28 wt% and 13.92 wt% for that of Fe_4Al_{13}. The different phase fraction in local regions reflects the inhomogeneous distribution of the large τ5c and Fe_4Al_{13} IMCs. In region 1, the phase fractions of τ5c and Fe_4Al_{13} contribute to nearly half of the alloy, while in region 2 there is a large amount of α-Al dendrite. It should be noted that the phase fraction obtained in Table 1 shows the weight percentage of the phases in nominal composition. In addition to the different phase fraction, the lattice parameter for α-Al, β-Zn, τ5c and Fe_4Al_{13} reveals the change of lattice in regions 1 and 2. When we compare the lattice parameters shown in Table 4, the values of the lattice parameters of α-Al, β-Zn and Fe_4Al_{13} for regions 1 and 2 are nearly identical, with only a negligible difference of approximately 0.1%. However, the lattice size of τ5c is noted to have a large difference with ~0.84% in the lattice size and ~2.5% in the unit cell volume. We speculate that this is likely to occur since the absorbed solutes in the IMC may result in changes in the lattice size because of differences in the different atomic sizes of the dissolved elements. In earlier studies [7,8] it has been confirmed that the ternary α-AlFeSi has a hexagonal unit cell; crystals with a cubic unit cell (with a lattice parameter of 12.56 Å) are formed only when a quaternary additions of transitions metals is made. The variations we observed the lattice parameters of the V-modified-τ5c IMC phase (12.55 Å in region 1 and 12.44 Å in region 2) may be attributed to the differing quantities of dissolved solutes in the IMC. It is plausible to assume that the dissolved solutes in the large lattices of the bcc structure may cause lattice shrinkage which may explain the differences between our results of the lattice parameter of the V-modified-τ5c IMC phase and that of the quaternary τ5c IMC phase.

Table 4.1. The fitting results of the lattice parameters for α-Al and β-Zn in the dross sample

Region	α-Al			β-Zn			
	Fm-3m			$P6_3/mmc$			
	a(Å)	V(Å^3)	PF (wt%)	a(Å)	c(Å)	V(Å^3)	PF (wt%)
1	4.0423(0)	66.052	42.89	2.6657(3)	4.9431(2)	30.421	22.03
2	4.0375(4)	65.819	68.22	2.6626(1)	4.9372(2)	30.313	12.79

Table 4.2. The fitting results of the lattice parameters for τ5c and q-Fe_4Al_{13} in the dross sample

	τ5c Im-3			Fe_4Al_{13} C2/m						R_{wp} (%)
	a(Å)	V(Å^3)	PF	a(Å)	b(Å)	c(Å)	β(°)	V(Å^3)	PF	
1	12.5472(4)	1975.353	22.03	15.3409(9)	8.0923(8)	12.4364(0)	107.19(7)	1474.897	27.28	8.98
2	12.4415(9)	1925.873	12.79	15.3234(8)	8.0686(4)	12.4040(9)	107.13(0)	1465.601	13.92	7.30

*PF: Phase Fraction (%)

4. The Substitution of Fe by V and the Periodic Layered Microstructure Formation Mechanism

To develop a conceptual framework for interpreting our observations, we plotted all the SEM/EDS line scan data of ((Fe+V)/Fe) for numerous dross particles, at reaction times ranging from 168 to 840 hours. The results of the analysis are summarized in Fig. 6. The ratio (Fe+V)/Fe represents the total number of atomic sites in the bcc structure of the IMC, both originally occupied by Fe and now substituted by V, relative to the original number of Fe sites. The ratio plotted against V (Fig. 6), gives a linear graph with an intercept of 1, implies that the number of atomic sites remains constant during the diffusion process. That is, for every atom of V that diffuses into the IMC and replaces an atom of Fe, the overall count of atoms in the structure does not change.

To further illustrate the fundamentals aspects of our observations and the periodic layered microstructure development, we introduce the concept of Newton's Cradle, as a suitable analogy to develop the conceptual framework. Newton's Cradle is a device used typically to demonstrate the conservation of momentum and energy. Newton's Cradle consists of a series of identical spheres suspended in a frame so that they are just touching each other at rest. If a sphere on one side is lifted and released, it strikes the next sphere in the row, sending the impact energy through the line of spheres. The sphere at the far end is then knocked away while the others remain in place. Using this analogy, we can think of the bcc structure of τ5c as the series of spheres.

That is, Fe represents the spheres at rest, while V represents the sphere that is lifted and released. The diffusion of V into τ5c is analogous to the energy transfer in the Newton's Cradle, with V taking the place of Fe without changing the overall structure, much like the far end sphere is knocked away in the cradle, but the overall structure remains the same. The constant linear relationship (Fig. 6) with an intercept of 1, indicates a conserved quantity: no matter how much of V diffuses into τ5c, the overall sum of Fe and V stays constant, much like the total energy in the Newton's Cradle. Let us illustrate this using SEM/EDS line scan data of Fig. 7:

· In the first layer: the initial motion starts with V = 1.97 diffusing into the layer which is followed by the displacement of Fe leading to an updated value of 17.88 at.% (note that τ5c contains ~19.85 at.% Fe). This is similar to the first sphere being lifted and released in Newton's Cradle. The (Fe+V)/Fe ratio for this layer is 1.11.

· Second layer: the displaced Fe from the first layer causes an increase in Fe in the second layer resulting in the new Fe value of 19.07 at.%. This is similar to the motion transferred from the first sphere to the second in newton's cradle. The ratio for this layer is 1.05.

· Third layer: the Fe displaced from the second layer increases Fe in the third layer resulting in the new Fe value of 18.43 at.%. This again mirrors the motion transfer from the second sphere to the third one in Newton's Cradle with a ratio of 1.1.

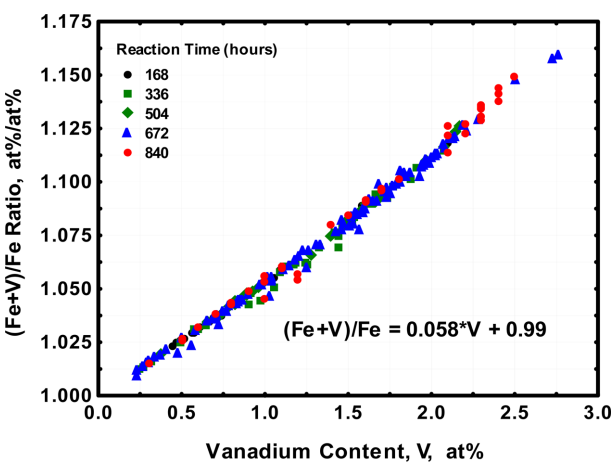

Fig. 6. Combined SEM/EDS line scan data of numerous dross particles at reaction times ranging from 168-840 hours

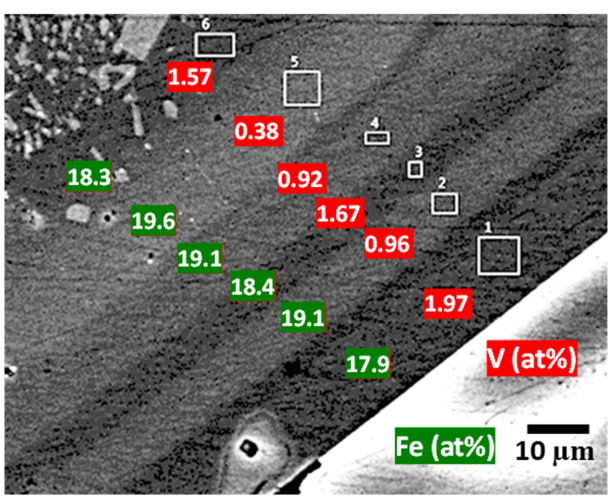

Fig. 7. The periodic layered structure from a dross particle after 504 hours of reaction in the bath.

· Fourth layer: the Fe displace from the third layer diffuses to the fourth layer, updating the Fe to 19.1 at.%. This reflects the motion transfer from the third to the fourth layer in the Newton's Cradle and the ratio for this layer is 1.05.

· Fifth layer: the Fe displaced from the fourth layer diffuses into the fifth layer, with Fe now at increasing to 19.6 at.% and the ratio for this layer is 1.02.

· Sixth layer: finally, the Fe displace from the fifth layer diffuses into the sixth layer, updating the Fe to 18.27 at.% with the ratio of 1.1 for the sixth layer.

5. Conclusions

1. We have experimentally confirmed vanadium can substitute for iron in τ5c-$Al_{20}Fe_5Si_2$(+Zn) intermetallic phase in 55%Al-Zn metal coating alloy. The substitution occurs without changes to the bcc crystal structure of the IMC.

2. Based on detailed microstructural characterization and SEM/EDS line scan data and the constancy of (Fe+V)/Fe ratio against V we propose a new theory for the formation of the periodic-layered microstructure observed in V modified τ5c intermetallic phase.

3. Using EBSD and micro-XRD the bcc crystal structure of the V-modified was confirmed. The bcc lattice parameters of the V-modified τ5c IMC and the lattice parameters the monoclinic Fe_4Al_{13} IMC phase was also determined.

4. At 600 ºC, the τ5c IMC phase can dissolve up to 4.13 wt% (2.73 at.%) vanadium.

Acknowledgement

We would like to thank our colleagues at BlueScope Innovating Labs for their engaging discussions during the course this work. We would also like to thank BlueScope Steel for permission to publish this work.

References

1. N Setargew, W. Y. D. Yuen and R. Chen, The reactivity of 316L stainless steel in 55%Al-Zn Bath, *Revue de Métallurgie*, **110**, 275 (2013). Doi: https://doi.org/10.1051/metal/2013069
2. D. Munson, A. Clarification of the phases occurring in aluminium-rich, aluminium-iron-silicon alloy with particular reference to the ternary phase Al-Fe-Si, *Journal of the Institute of Metals*, **95**, 217 (1967).
3. D. J. Skinner, R. L. Bye, D. Raybold and A. M. Brown, Dispersion strengthened Al-Fe-V-Si alloys, *Scripta Metallurgica*, **20**, 867 (1986). Doi: https://doi.org/10.1016/0036-9748(86)90456-4
4. J. Q. Wang, C. F. Qian, B. J. Zhang, M. K. Tseng, and S. W. Xiong, Valence electron structure analysis of the cubic silicide intermetallic in rapidly solidified Al-Fe-V-Si alloy, *Scripta Materialia*, **34**, 1509 (1996). Doi: https://doi.org/10.1016/1359-6462(96)00002-4
5. N. Setargew, D. J. Willis, and A. Dixon, Spangle nucleation and refinement theory in 55%Al-Zn coated steel, *Proc. 12th International Conference on Zinc and Zinc Alloy Coated Sheet Steel*, (Galvatech 2021), p. 1291, Vienna, Austria (2021).
6. M. Cooper, The crystal structure of the ternary alloy α (AlFeSi), *Acta Crystallogr.*, **23**, 614 (1967).
7. T. Turmezey, V. Stefániay, and A. Griger, *Effect of Iron and Silicon in Aluminium and Its Alloys*, *Proc. of Int. Workshop*, Held in Balatonfüred, Hungry (1989).
8. J. N. Pratt, and V. G. Raynor, The intermetallic compounds in the alloys of aluminium and silicon with chromium, manganese, iron, cobalt, and nickel, *Journal of the Institute Metalls*, **79**, 211 (1951).